NASA TECHNICAL NOTE

NASA TN D-3424


NASA TN D-3424



# ANALYSIS OF n-HEPTANE VAPORIZATION IN UNSTABLE COMBUSTOR WITH TRAVELING TRANSVERSE OSCILLATIONS

*by Marcus F. Heidmann and Paul R. Wieber*

*Lewis Research Center*
*Cleveland, Ohio*

NATIONAL AERONAUTICS AND SPACE ADMINISTRATION • WASHINGTON, D. C. • MAY 1966

NASA TN D-3424

# ANALYSIS OF n-HEPTANE VAPORIZATION IN UNSTABLE COMBUSTOR WITH TRAVELING TRANSVERSE OSCILLATIONS

By Marcus F. Heidmann and Paul R. Wieber

Lewis Research Center
Cleveland, Ohio

NATIONAL AERONAUTICS AND SPACE ADMINISTRATION

For sale by the Clearinghouse for Federal Scientific and Technical Information
Springfield, Virginia 22151 – Price $2.00

# ANALYSIS OF n-HEPTANE VAPORIZATION IN UNSTABLE COMBUSTOR WITH TRAVELING TRANSVERSE OSCILLATIONS*

by Marcus F. Heidmann and Paul R. Wieber

Lewis Research Center

## SUMMARY

Vaporization histories of n-heptane drops in a combustor with superimposed traveling transverse oscillations were computed by using drop-evaporation theory. Oscillations in the rates of vaporization of an array of repetitively injected drops in the combustor were obtained from summations of individual drop histories. A frequency response of the entire vaporization process to oscillations in pressure was evaluated. The typical response curve showed a maximum value at a specific frequency. The response factor approached zero at lower frequencies and a constant negative value at higher frequencies, which indicated a potential for both the driving and damping of acoustic oscillations.

Changes in combustor and drop parameters were investigated. The critical frequency, which divided regions of positive and negative response, increased with an increase in combustor pressure, combustor axial gas velocity, and amplitude of the pressure oscillations. It decreased with an increase in drop radius. Changes in initial drop velocity and temperature caused no significant change in critical frequency. An evaluation of liquid-oxygen vaporization showed propellant properties to be important.

A normalized response characteristic based on a correlation of vaporization parameters is presented. The correlation shows that the peak response occurs when a drop is vaporized in a time period approximately equal to the oscillation period. Negative gains occur when the vaporization time is greater than about three times the oscillation period. Drop lifetimes less than three times the oscillation period are frequently encountered in unstable rocket combustors.

---

*Part of the material given herein was presented at the Second Combustion Instability Conference, Los Angeles, California, Nov. 1-5, 1965.

# INTRODUCTION

System analyses of unstable combustion (refs. 1 and 2) have shown that propellant vaporization is a process which, when varied, can control system stability. In such system analyses, the dynamic response of the rate of propellant vaporization to the acoustic pressure oscillations is not readily identified. It is the purpose of this report to evaluate the response characteristic for a range of conditions in vaporization parameters. The evaluations provide a measure of the sensitivity of the vaporization process to acoustic oscillations by indicating its driving or damping potential in an unstable feedback loop.

The drop vaporization theory, developed in reference 3 to evaluate combustor performance for a vaporization-limited combustion process, is used in this study to compute drop vaporization histories in a rocket combustor with superimposed acoustic oscillations. In the vaporization calculations, the acoustic oscillations affect the drop acceleration and heat and mass transfer processes by giving the drop three-dimensional velocity components and causing perturbations in drop temperature and evaporation rate. With these variations, the rate of vaporization depends on the frequency of the oscillation, and a frequency response can be evaluated. This application of the theory differs from that used in the system analyses of references 1 and 2, where the vaporization rate varied only with perturbations in drop Reynolds number about a mean condition in vaporization and was independent of the frequency of the oscillations.

Calculations are made for n-heptane drops vaporizing in a cylindrical combustor containing heptane-oxygen combustion products. Pressure, velocity, and temperature oscillations, associated with the first traveling transverse acoustic mode, are superimposed on the normal combustion flow process. Individual drop histories are obtained for boundary conditions which include changes in combustor pressure, final combustion gas velocity, drop radius, initial drop velocity, initial drop temperature, drop radial position in the combustor, and the amplitude and frequency of the acoustic mode. An evaluation of oxygen vaporization is made to explore the effects of propellant properties on vaporization in an acoustic field.

Individual drop histories depend on the time and position of drop injection into the combustor with respect to the orientation of the acoustic mode. A summation of these individual histories is used to obtain the time variations in the vaporization rate of repetitively injected drops throughout the combustor. The summation provides a response of the entire vaporization process treated as an entity. This response factor is expressed as the ratio of the percentage oscillation in vaporization rate to the percentage oscillation in pressure and accounts for phase relations. Variations in the response factor with frequency and boundary condition are presented.

# SYMBOLS

| | |
|---|---|
| $\mathscr{A}$ | contraction ratio, dimensionless |
| a | speed of sound, ft/sec |
| $c_p$ | specific heat, Btu/(lb)($^{\circ}$R) |
| $D_v$ | diffusivity, $ft^2$/sec |
| F | transformed frequency, $f\left[\left(\frac{R_{d,0}}{50}\right)^{3/2}\left(\frac{300}{P_c}\right)^{1/3}\left(\frac{800}{U_F}\right)^{1/3}\left(\frac{0.2}{\Delta P_c/P_c}\right)^{1/3}\right]$, cps |
| f | frequency, cps |
| $H_v$ | heat of vaporization, Btu/lb |
| $J_i$ | Bessel function of order i |
| k | thermal conductivity, Btu/(ft)(sec)($^{\circ}$R) |
| L | length of combustion zone, ft |
| $\mathscr{L}$ | burning rate parameter, dimensionless |
| $M_F$ | final Mach number, $U_F/a$, dimensionless |
| $\mathscr{M}$ | molecular weight, lb/lb mole |
| $\dot{m}$ | fraction of weight burned or vaporized per unit length, $ft^{-1}$ |
| N | response factor, $(\Delta\dot{W}/\dot{W})/(\Delta P_c/P_c)$, dimensionless |
| n | interaction index (see ref. 6) |
| $P_c$ | average gas pressure, $lb/in.^2$ |
| $P_L$ | vapor pressure at liquid surface, $lb/ft^2$ |
| Pr | Prandtl number, $(c_{p,m}\mu_m)/k_m$ |
| $P_T$ | total gas pressure, $144(P_c + \tilde{P}_c)$, $lb/ft^2$ |
| $\Delta P_c$ | maximum peak-to-peak pressure oscillation in combustor, $lb/in.^2$ |
| R | gas constant, (ft)(lb)/(lb mole)($^{\circ}$R) |
| $R_d$ | drop radius, ft |
| $R_{d,0}$ | initial drop radius, microns |
| Re | Reynolds number, $(2R_d\rho_m \Delta V)/\mu_m$ |
| $R_w$ | combustor radius, ft |
| r | drop radial position, ft |

| | |
|---|---|
| Sc | Schmidt number, $\mu_m/D_v\rho_m$ |
| $T_c$ | gas temperature associated with average gas pressure, $^oR$ |
| $T_L$ | drop temperature, $^oR$ |
| $T_T$ | total gas temperature, $T_c + \tilde{T}_c$, $^oR$ |
| t | time, sec |
| $t_\sim$ | cycle time, 1/f, sec |
| U | axial gas velocity, ft/sec |
| $U_d$ | axial drop velocity, ft/sec |
| $U_F$ | final axial gas velocity, ft/sec |
| V | transverse gas velocity, ft/sec |
| $V_d$ | transverse drop velocity, ft/sec |
| $\Delta V$ | vector sum of all directional components of velocity difference between gas and drop, $\left[(U - U_d)^2 + (V_r - V_{d,r})^2 + (V_\theta - V_{d,\theta})^2\right]^{1/2}$, ft/sec |
| $\dot{W}$ | vaporization rate of drop array, lb/sec |
| w | drop weight, lb |
| $\dot{w}$ | vaporization rate of single drop, lb/sec |
| $\gamma$ | ratio of specific heats, dimensionless |
| $\theta$ | drop angular position, radians |
| $\mu$ | viscosity, lb/(ft)(sec) |
| $\rho$ | density, $lb/ft^3$ |
| $\tau$ | characteristic time (see ref. 6), sec |

Subscripts:

| | |
|---|---|
| L | liquid value |
| m | mean value based on film composition and/or temperature |
| peak | frequency at which response factor reaches maximum |
| r | radial component |
| v | vapor value |
| $\theta$ | angular component |
| 0 | initial value |

50 value when 50 percent of drop mass is evaporated

Superscripts:

$\sim$ perturbation component

$\cdot$ rate with respect to time

$-$ average

## METHOD OF ANALYSIS

The technique used herein is described in two parts. The first part presents the assumptions in the model and lists the equations which are solved to give single drop histories. By means of a sample calculation, the second part depicts the use of single drop histories in generating the vaporization response factor for a column of repetitively injected drops exposed to an acoustic oscillation.

### Vaporization Model

Drops of n-heptane are assumed to be vaporizing in combustion gases, composed of stoichiometric reaction products with oxygen in a cylindrical combustor, with an established traveling-transverse resonant acoustic mode. The pressure and gas velocity oscillations attributed to the acoustic mode are derived from the relations in references 4 and 5:

$$\frac{\tilde{P}_c}{P_c} = 0.859 \frac{\Delta P_c}{P_c} \left( J_1 \frac{1.841\ r}{R_w} \right) \sin(2\pi ft - \theta) \tag{1}$$

$$\tilde{V}_r = 0.430 \frac{a}{\gamma} \frac{\Delta P_c}{P_c} \left( J_0 \frac{1.841\ r}{R_w} - J_2 \frac{1.841\ r}{R_w} \right) \cos(2\pi ft - \theta) \tag{2}$$

$$\tilde{V}_\theta = 0.467 \frac{a}{\gamma} \frac{R_w}{r} \frac{\Delta P_c}{P_c} \left( J_1 \frac{1.841\ r}{R_w} \right) \sin(2\pi ft - \theta) \tag{3}$$

The wave is assumed to be adiabatic with

$$\frac{\tilde{\rho}_c}{\rho_c} = \left(\frac{\tilde{P}_c}{P_c}\right)^{1/\gamma} \tag{4}$$

$$\frac{\tilde{T}_c}{T_c} = \left(\frac{\tilde{P}_c}{P_c}\right)^{(\gamma-1)/\gamma} \tag{5}$$

The oscillations are superimposed on the mean level of the parameters affecting drop evaporation and motion. In the theory of reference 3 used in this study, vaporization rate is controlled by heat and mass transfer at the drop surface. Drop motion is obtained from a momentum balance in three vector directions. Axial gas velocity is proportional to the fraction of drop mass vaporized, and it attains a final assumed velocity at complete vaporization.

The drop history is described by following equations for weight evaporation rate, heating rate, and acceleration in an axial direction. The weight evaporation rate can be defined as

$$\dot{w} = \frac{2\pi R_d D_v \mathcal{M}_L}{R} \frac{P_T}{T_m} \left[\ln\left(\frac{P_T}{P_T - P_L}\right)\right](2 + 0.6\ Sc^{1/3}Re^{1/2}) \tag{6}$$

The heating rate $\dot{T}_L$ is found by

$$\dot{T}_L = \frac{3}{2C_{p,L}\rho_L R_d^2} \left\{k_m(T_T - T_L) \frac{z}{e^z - 1} (2 + 0.6\ Pr^{1/3}Re^{1/2}) \right.$$

$$\left. - \frac{D_v \mathcal{M}_L H_v}{R} \frac{P_T}{T_m} \left[\ln\left(\frac{P_T}{P_T - P_L}\right)\right](2 + 0.6\ Sc^{1/3}Re^{1/2})\right\} \tag{7}$$

where

$$z = \frac{D_v \mathcal{M}_L C_{p,v}}{R k_m} \frac{P_T}{T_m} \left[\ln\left(\frac{P_T}{P_T - P_L}\right)\right] \frac{2 + 0.6\ Sc^{1/3}Re^{1/2}}{2 + 0.6\ Pr^{1/3}Re^{1/2}} \tag{8}$$

The final equation necessary for describing the drop history is that of acceleration in an axial direction, which is

$$\dot{U}_d = 5.656 \frac{\rho_m^{0.16} \mu_m^{0.84}}{\rho_L R_d^{1.84}} \Delta V^{0.16} (U - U_d) \tag{9}$$

Similar equations can be written for the Cartesian components of the two transverse drop accelerations $\dot{V}_{d,r}$ and $\dot{V}_{d,\theta}$, where the quantity $U - U_d$ is replaced by the transverse relative velocity between the gas and the drop and transformed into corresponding Cartesian coordinates. The axial gas velocity is given by

$$U = U_F \left(1 - \frac{w}{w_0}\right) \tag{10}$$

Liquid and gas properties were taken from equations in references 3 and 6 plus curve fits of data for heat of vaporization, vapor pressure, and liquid density. Direct analytical solutions are not possible, and evaluations are obtained by numerical techniques which employ a high-speed digital computer.

## Vaporization Histories

The dynamic behavior of the entire vaporization process is obtained from a summation of instantaneous values in the vaporization histories of individual drops. This is best described by the procedure for a specific set of boundary conditions. The example chosen is for drops of 50-micron radius injected at a velocity of 100 feet per second and an initial temperature of $650^{\circ}$ R. Mean combustor pressure is 300 pounds per square inch, and the final gas velocity attains a value of 800 feet per second. The acoustic oscillation has a peak-to-peak pressure amplitude of 20 percent of combustor pressure at a frequency of 3000 cps. Drop vaporization histories with these boundary conditions depend on two variables: (1) the phase time of drop injection with respect to the oscillation in pressure, and (2) the radial position of injection within the cross section of the combustor. Since the acoustic mode has traveling wave properties, these two variables are sufficient to specify the vaporization of any drop injected into the combustor.

The vaporization histories of an array of continuously injected drops at a radial position $r/R_w$ of 0.912 will be considered first. Figure 1 shows the vaporization history of a drop injected at the mean pressure preceding a rise in oscillatory pressure ($2\pi ft - \theta = 0$ in eqs. (1) to (3)). Vaporization rates, in addition to other combustor parameters, are shown as a function of cycle time. For comparison, the vaporization history without acoustic oscillations is also shown. Although the oscillation substantially

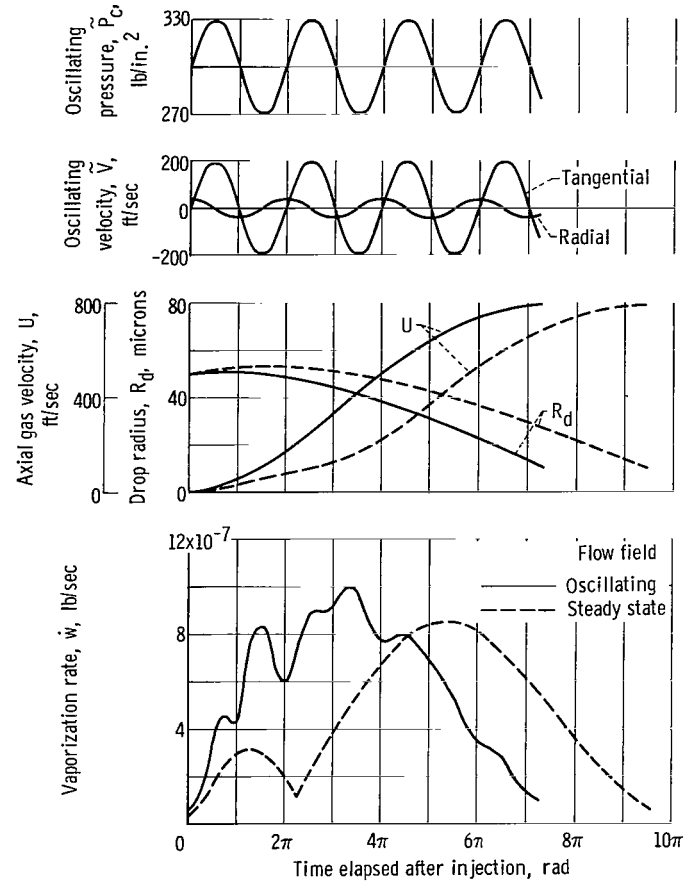


Figure 1. - Time histories of drop and combustor parameters in steady-state and oscillating flow field. Drop conditions: radius, 50 microns; velocity, 100 feet per second; temperature, 650° R; radial position, 0.912 of combustor radius. Gas conditions: pressure, 300 pounds per square inch; final velocity, 800 feet per second; oscillation frequency, 3000 cps; oscillation peak-to-peak amplitude, 0.2 of average gas pressure.

reduces the total time for vaporization, the characteristic of interest in this study is the oscillation in vaporization rate. Oscillations in vaporization rate occur at twice the frequency of the pressure oscillations. This rectified-type response is caused by the sensitivity of the vaporization process to the absolute velocity difference between the drop and combustion gases. Velocity difference reaches a maximum twice during each pressure oscillation and never becomes equal to zero because the two transverse gas velocity components have a $90^{\circ}$ phase difference.

## Summation of Histories

A specific summation of single-drop histories is used to evaluate the time variations

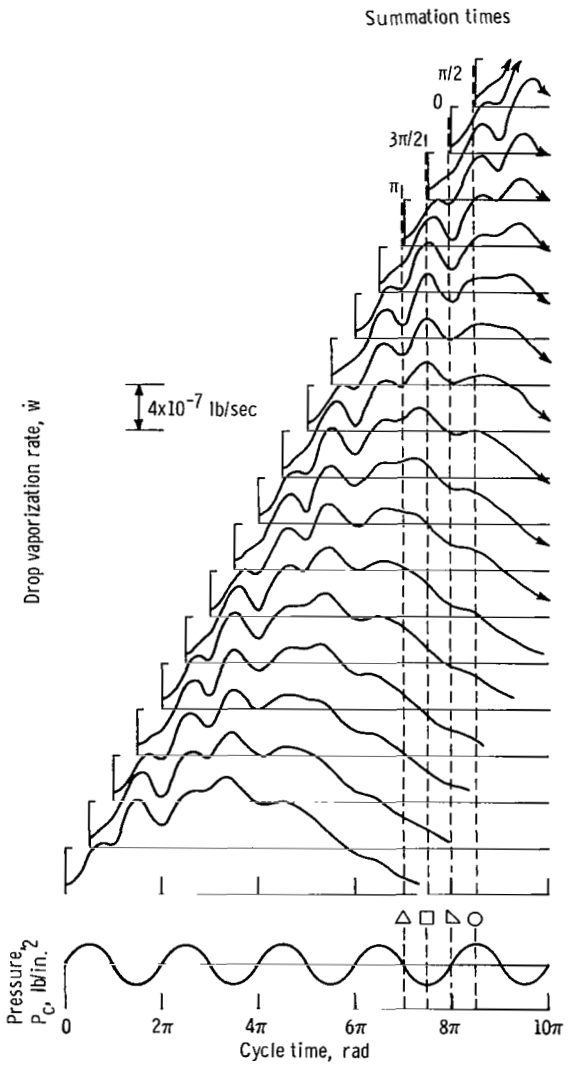


Figure 2. - Generation of array of drops from individual drop histories. Drop conditions: radius, 50 microns; velocity, 100 feet per second; temperature, 650° R; radial position, 0.912 of combustor radius. Gas conditions: pressure, 300 pounds per square inch; final velocity, 800 feet per second; oscillation frequency, 3000 cps; oscillation peak-to-peak amplitude, 0.2 of average gas pressure. Each vaporization curve begins at zero point.

in vaporization rate of a one-dimensional array of repetitively injected drops. The drop histories in figure 2 illustrate the summation.

Figure 2 shows vaporization rate histories for drops injected at a fixed radial and angular position in the combustor. Drop histories displayed along the ordinate are related to the cycle time of the acoustic oscillation along the abscissa. The pressure oscillation is shown along the abscissa for reference.

Four drops are injected every cycle at the four cycle times of 0, $\pi/2$, $\pi$, and $3\pi/2$. Vaporization histories vary among drops injected at different times during one pressure oscillation, as shown by the first four histories. However, drops injected at times $2\pi$ apart experience identical acoustic pressure and velocity fields and, thus, have identical histories. Eventually, the same number of drops are completely vaporized per cycle as are injected, and the number of drops in the array becomes constant over each full cycle. For the example illustrated, the fully developed array contains 15 drops, decreasing in mass down the chamber and ranging in age from a new drop just injected to an old one almost completely vaporized. With the array fully developed, the distribution of vaporization rates along the array can be obtained at any time during the oscillation in pressure. This is done in the example at cycle times of $\pi$, $3\pi/2$, 0, and $\pi/2$, as indicated by the vertical dashed lines of figure 2.

The mass vaporizing from the entire array of drops at each specific cycle time is the summation of that vaporizing from all the individual drops.

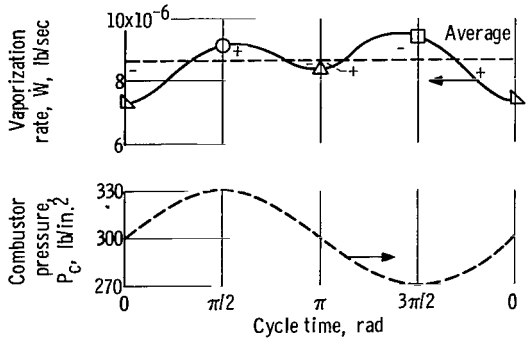


Figure 3. - Vaporization rates of array of continuously injected drops during oscillation in pressure. Drop conditions: radius, 50 microns; velocity, 100 feet per second; temperature, 650° R; radial position, 0.912 combustor radius. Gas conditions: pressure, 300 pounds per square inch; final velocity, 800 feet per second; oscillation frequency, 3000 cps; oscillation peak-to-peak amplitude, 0.2 of average gas pressure.

$$\dot{W} = \sum_{i} \dot{w}_i \qquad (11)$$

This summation is plotted as a function of cycle time in figure 3. The curve of figure 3 is the response of the vaporization rate of the array to an acoustic oscillation. The average of all the summations over a complete cycle is also shown. The effect of angular and radial displacement of the drop in the chamber due to the oscillating flow field was small and was neglected in relating the phase of vaporization rate and pressure. The vaporization rate is higher throughout the array at both the maximum and minimum pressure condition in the oscillation than at the mean pressure conditions. Lower rates occur at mean pressure because the total velocity is a minimum at the mean pressure in a traveling wave.

The example was simplified for clarity. In actual computation, the response curve was improved in two ways. First, the minimum number of drop histories that would give an acceptable summation was set at 16 to improve the average value. For the boundary conditions of the example case, this was obtained by injecting eight drops per cycle instead of four. Thus, the number of drops injected per cycle was dependent on the drop lifetime and the period of the oscillation. Second, the continuity of the curve was improved by sampling the array at 16 cycle times for all cases instead of only 4 times as shown.

## Response Factor

The response curve of figure 3 shows that a sinusoidal oscillation in pressure causes an oscillation in vaporization rate which exhibits harmonic components of the basic frequency. The relation between pressure and vaporization rate, therefore, cannot be expressed simply by a gain and phase angle, as is frequently done in dynamic analysis.

A response factor (effective gain), which combines the amplitude ratio and phase relation of vaporization rate and oscillation pressure in a single quantity, was numerically evaluated. This response factor is assumed positive when vaporization rate and chamber pressure are both above or below their mean values and assumed negative when vaporization rate and chamber pressure are on opposite sides of their means. This is applied throughout the cycle. The regions where the response factors are positive and negative

are indicated in figure 3. When this convention is used, the response factor for the entire oscillation can be expressed by the ratio

$$N = \frac{\frac{\Delta \dot{W}}{\dot{W}}}{\frac{\Delta P_c}{P_c}} \tag{12}$$

The vaporization term is expressed by the summation

$$\frac{\Delta \dot{W}}{\dot{W}} = \frac{\sum_{0}^{\pi} \left( \dot{W} - \overline{\dot{W}} \right) + \sum_{\pi}^{2\pi} \left( \overline{\dot{W}} - \dot{W} \right)}{\sum_{0}^{2\pi} \dot{W}} \tag{13}$$

and the pressure term is defined by a similar summation, evaluated in all cases for the maximum pressure amplitudes that occur at the combustor wall.

The response factor is an index of the degree of driving or damping which the vaporization process provides in a feedback loop, as generally postulated for combustion instability (ref. 7). It is comparable to the pressure exponent in a linearization of

$$\dot{W} \sim P_c^N \tag{14}$$

where

$$N = \frac{\frac{d\dot{W}}{\dot{W}}}{\frac{dP_c}{P_c}} \tag{15}$$

The response factor in this example is -0. 177. Vaporization rate contributes to negative feedback when rate and pressure are interrelated. The value applies to all angular positions at 0. 912 of the maximum radius. It is independent of angular position because of the traveling wave characteristics of this transverse mode.

TABLE I. - RANGE OF BOUNDARY CONDITIONS

[Combustor temperature, $T_c$, 5000° R.]

| Combustor pressure, $P_c$, lb/in.$^2$ | Final axial gas velocity, $U_F$, ft/sec | Initial axial drop velocity, $U_{d,0}$, ft/sec | Initial drop temperature, $T_{L,0}$, °R |
|---|---|---|---|
| 150 | [a]800 | [a]100 | [a]650 |
| [a]300 | [a]800 | | |
| 600 | [a]800 | | |
| [a]300 | 400 | | |
| | 2400 | | |
| | [a]800 | 50 | |
| | | 200 | |
| | | [a]100 | 500 |
| | | [a]100 | 800 |

[a]Boundary conditions of reference case.

## Area Average

The response factor varies with radial position because of the changes in pressure and velocity oscillations specified by equations (1) to (3). Pressure oscillations for this mode of resonance vanish at the axis of the combustor, although velocity oscillations persist throughout the combustor. A response factor, which accounts for this effect, is obtained from an average of the response factors at three radial positions. The three radial positions are the mean radii of three concentric equal areas. These radii are 0.912, 0.707, and 0.409 of the maximum radius.

## Range of Boundary Conditions

By using the ideas just presented, the response of the entire vaporization process is evaluated for the range of boundary conditions shown in table I. These boundary conditions survey the effect of combustor pressure, final gas velocity, initial drop radius, velocity, temperature, radial injection position, and the amplitude of the pressure oscillation. Pressure amplitude ratio is given at the circumference of the combustor, where it is a maximum.

For table I, calculations were made for all combinations (approximately 600) of the following:

Drop radius, $R_{d,0}$, microns . . . . . [†]50, 150, 500
Pressure amplitude ratio, $\Delta P_c/P_c$ . . . . . 0.1, [†]0.2, 0.4
Radial position, $r/R_w$ . . . . . 0.409, 0.707, 0.912
Frequency, f, cps . . . . . 100, 300, 500, 1000, 3000, 10 000

The effect of propellant properties was explored by evaluating several cases of liquid-oxygen vaporization at selected boundary conditions.

[†]Boundary conditions of reference case.

## RESULTS AND DISCUSSION

The variation in response factor with frequency is defined as the frequency response of the vaporization process. The effect of boundary conditions, illustrated in figures 4 to 10, was obtained from a parametric study of the reference boundary conditions, as indicated in table I. Reference boundary conditions include the following: drop radius, 50 microns; combustor pressure, 300 pounds per square inch; pressure amplitude ratio, 0.2; final axial gas velocity, 800 feet per second; initial axial drop velocity, 100 feet per second; and initial drop temperature, $650^{\circ}$ R.

### Radial Position

The frequency response for the reference boundary conditions is shown in figure 4. The response at the three radial positions and the average for the entire vaporization process are shown. These frequency response characteristics are typical for all conditions. The response factor exhibits a positive maximum, or peak, value at a specific frequency. It approaches zero at a lower frequency and decreases to a negative value at higher frequencies. This behavior is characteristic of a damped resonant system, where a peak response occurs at some frequency and a negative feedback occurs at a higher frequency. If this behavior is realistic, it is significant to the problem of combustion instability in rocket combustors. It implies that the vaporization process may be tuned to the acoustic frequency of the combustion cavity.

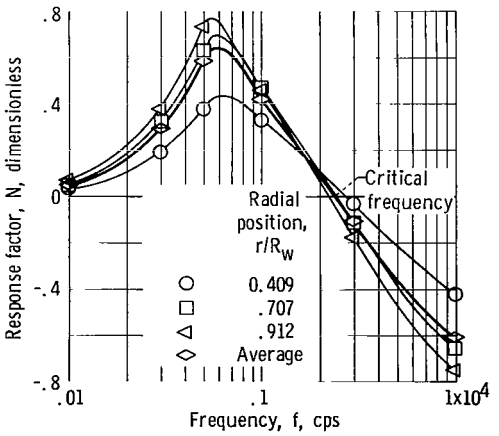


Figure 4. - Frequency response at three radial positions. Drop conditions: radius, 50 microns; velocity, 100 feet per second; temperature, $650^{\circ}$ R. Gas conditions: pressure, 300 pounds per square inch; final velocity, 800 feet per second; oscillation peak-to-peak amplitude, 0.2 of average gas pressure.

In general, larger positive and negative response factors were observed as radial position approached the combustor wall. The frequency for peak or maximum response, however, is relatively unaffected. The average response factor for the entire vaporization process is approximately the same as that for the 0.707 radial position, which divides the combustor into equal concentric areas.

A maximum response factor of 0.76 is obtainable at a radial position of 0.912. In a resonant system, where acoustic energy may accumulate, self-sustained oscillations are possible with a response factor greater than zero (the exact value depending on losses). A response factor less than zero will always introduce damping into a system.

The frequency for a zero response factor, therefore, divides the frequency response into regions of driving and damping and may be considered a critical frequency. It is shown to be about 2500 cps for the average response curve at the reference boundary conditions. This frequency provides a point of comparison in evaluating the effect of boundary conditions on frequency response.

## Drop Size

The effect of increasing drop radius from 50 to 500 microns is shown in figure 5. The critical frequency, as previously defined, decreases with an increase in drop size. The response factor approaches the same constant negative value independent of size. The effect of drop size is principally a frequency displacement of the response curve. A peak response at about 100 cps is shown for 150-micron drops, and presumably, a peak for 500-micron drops exists at a lower frequency.

## Combustor Pressure

A change in mean combustor pressure affects the response, as shown in figure 6. Increasing pressure increases the critical frequency and also gives a higher peak response. This reflects the increase in both acceleration forces and thermal driving force

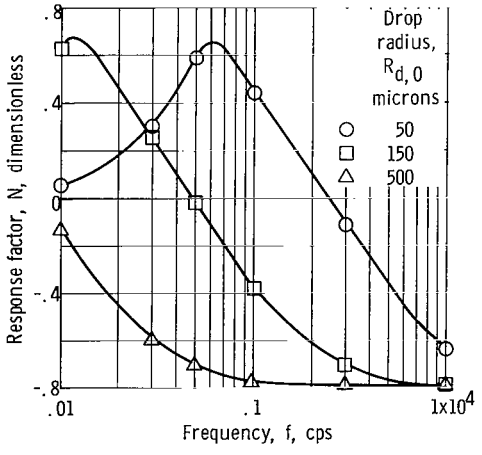


Figure 5. - Effect of initial drop radius. Drop conditions: velocity, 100 feet per second; temperature, 650° R. Gas conditions: pressure, 300 pounds per square inch; final velocity, 800 feet per second; oscillation peak-to-peak amplitude, 0.2 of average gas pressure.

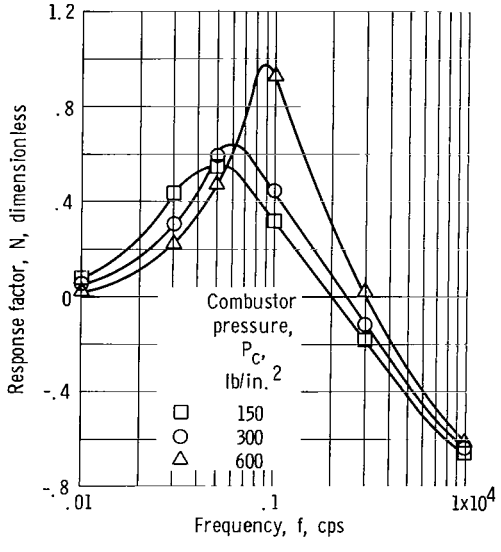


Figure 6. - Effect of combustor pressure. Drop conditions: radius, 50 microns; velocity, 100 feet per second; temperature, 650° R. Gas conditions: final velocity, 800 feet per second; oscillation peak-to-peak amplitude, 0.2 of average gas pressure.

with pressure and also the change in properties as the drop heats to higher temperatures at higher pressures. It also may reflect a limitation of the analytical model. When drop temperatures approach the thermodynamic critical temperature, vaporization rate is accelerated, but the accuracy of the analytical expressions becomes uncertain (ref. 6). Oscillations in pressure, superimposed on the high chamber pressure, may have caused the drops to approach this region of accelerated vaporization and, thus, given an uncertain peak value.

## Final Gas Velocity

Response curves for final gas velocities of 400, 800, and 2400 feet per second are shown in figure 7. Final gas velocities of this magnitude are reached in combustors with contraction ratios of about 6, 3, and 1.5, respectively. Increasing final gas velocity increases the critical frequency, but it has little effect on the shape of the response curve.

## Initial Drop Velocity

Initial drop velocity has a negligible effect on frequency response, as shown in figure 8 for injection velocities of 50, 100, and 200 feet per second. An increase in initial drop velocity decreases the distance for complete vaporization in steady combustion (ref. 3), but it appears to have little effect on the time-dependent properties evaluated in this study.

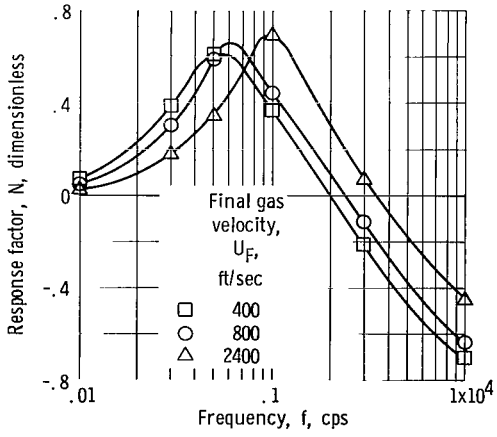


Figure 7. - Effect of final gas velocity. Drop conditions: radius, 50 microns; velocity, 100 feet per second; temperature, 650° R. Gas conditions: pressure, 300 pounds per square inch; oscillation peak-to-peak amplitude, 0.2 of average gas pressure.

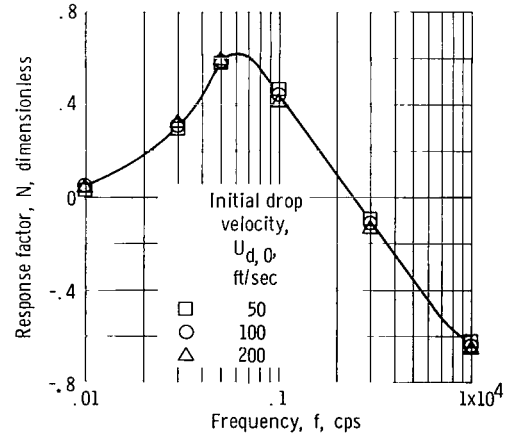


Figure 8. - Effect of initial drop velocity. Drop conditions: radius, 50 microns; temperature, 650° R. Gas conditions: pressure, 300 pounds per square inch; final velocity, 800 feet per second; oscillation peak-to-peak amplitude, 0.2 of average gas pressure.

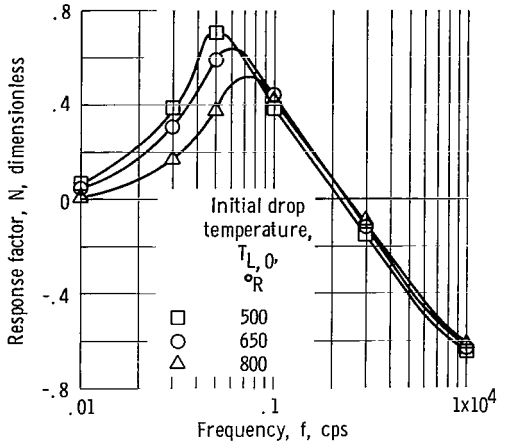


Figure 9. - Effect of initial drop temperature Drop conditions: radius, 50 microns; velocity, 100 feet per second. Gas conditions: pressure, 300 pounds per square inch; final velocity, 800 feet per second; oscillation peak-to-peak amplitude, 0.2 of average gas pressure.

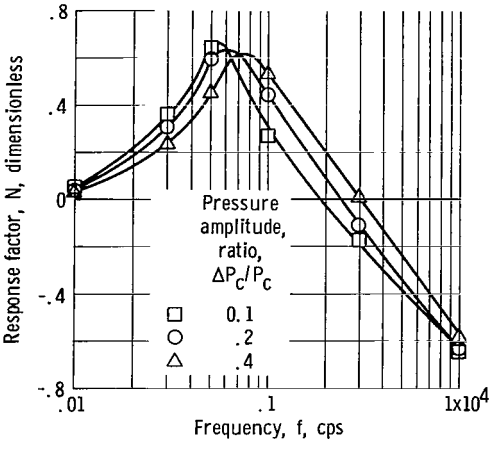


Figure 10. - Effect of peak-to-peak pressure amplitude ratio. Drop conditions: radius, 50 microns; velocity, 100 feet per second; temperature, 650° R. Gas conditions: pressure, 300 pounds per square inch; final velocity, 800 feet per second.

## Initial Drop Temperature

The effect of changes in initial drop temperature from $500^{\circ}$ to $800^{\circ}$ R is shown in figure 9. Drop injection temperature affects the magnitude of the response factor only at low frequencies, but it has no appreciable effect on the critical frequency. Peak positive response factors increase with a decrease in initial temperature.

## Pressure Amplitude

Figure 10 shows that peak-to-peak pressure amplitude ratios of 0.1, 0.2, and 0.4 have a small effect on the magnitude of the response factor; the critical frequency, however, increases with an increase in wave amplitude. This characteristic indicates a changing frequency response during the buildup period of pressure oscillations in an unstable combustor.

## Propellant Properties

The frequency response for liquid oxygen drops vaporizing in combustion gases composed of stoichiometric reaction products with hydrogen was evaluated at the reference boundary conditions used for heptane vaporization but with an injection temperature of

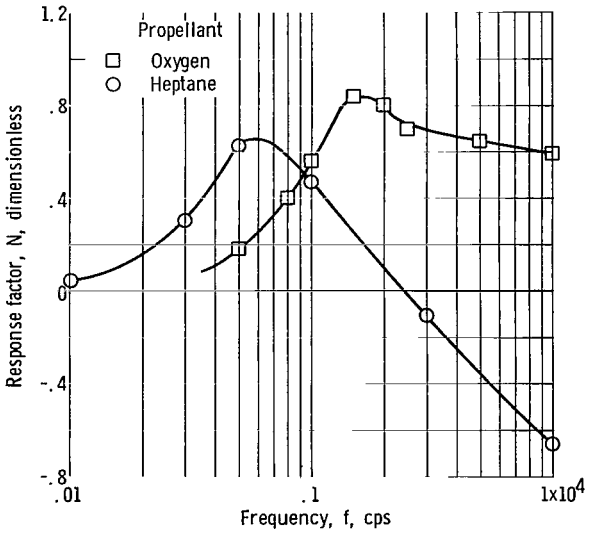


Figure 11. - Effect of propellant properties. Drop conditions: radius, 50 microns; velocity, 100 feet per second; heptane temperature, 650° R; oxygen temperature, 140° R; radial position, 0.707 of combustor radius. Gas conditions: pressure, 300 pounds per square inch; final velocity, 800 feet per second; oscillation peak-to-peak amplitude, 0.2 of average gas pressure.

140° R. This exploration of the effect of propellant properties is shown in figure 11. The significant differences in the frequency response for oxygen compared with heptane are the larger peak values of the response factor and the absence of a region of negative response factor. This comparison shows that propellant properties can have a significant effect on frequency response of a vaporization process.

## Correlation of Results

The frequency response curves for heptane vaporization were combined to obtain a single curve representing the results for the range of boundary conditions evaluated in this study. The curves were combined by a transformation in frequency, as shown in figure 12 (p. 18). The transformed frequency giving this correlation of results is

$$F = f\left(\frac{R_{d,0}}{50}\right)^{3/2}\left(\frac{300}{P_c}\right)^{1/3}\left(\frac{800}{U_F}\right)^{1/3}\left(\frac{0.2}{\frac{\Delta P_c}{P_c}}\right)^{1/3} \tag{16}$$

At the critical frequency, F is 2500 cps. The factor is normalized to the reference set of boundary conditions to facilitate numerical evaluations.

The complete range of boundary conditions correlates with the frequency factor to within a relatively small deviation. Figure 13 shows, by the shaded area, the range of deviation within which all the results fall. The greatest deviation exists at the peak values. A single curve, however, is adequate to represent the frequency response to within the accuracy expected for the analytical model and method of evaluation.

The curve is applicable only to heptane vaporization with traveling transverse acoustic oscillations. Other modes, principally standing, prescribe relations between pres-

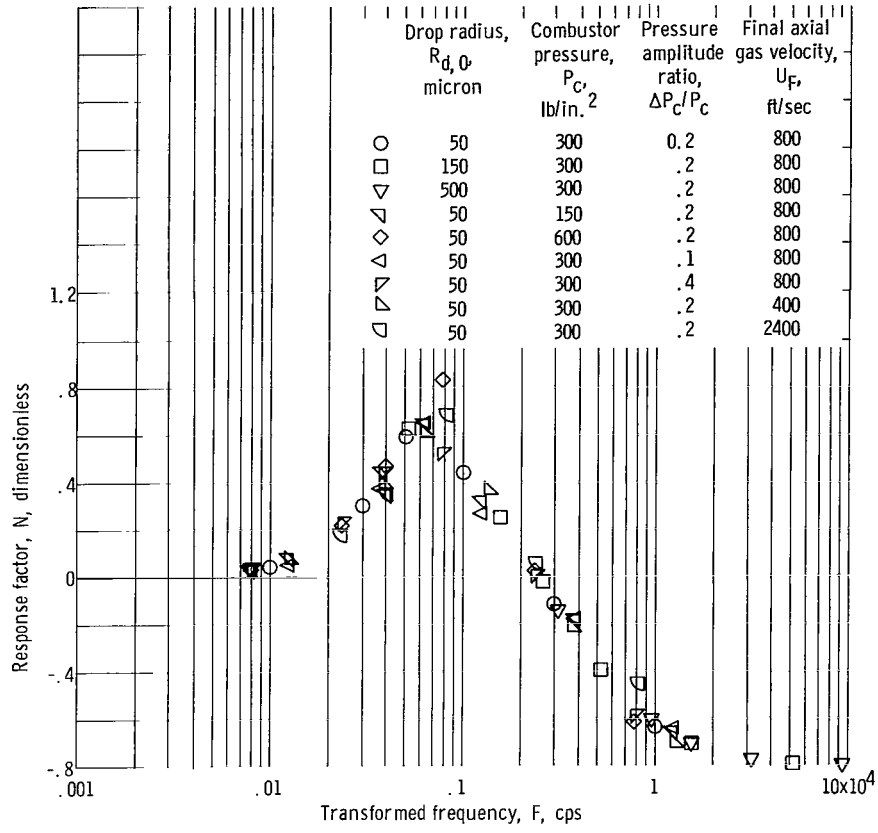


Figure 12. - Correlation of representative heptane results. Initial axial drop velocity, 100 feet per second; initial drop temperature, 650° R.

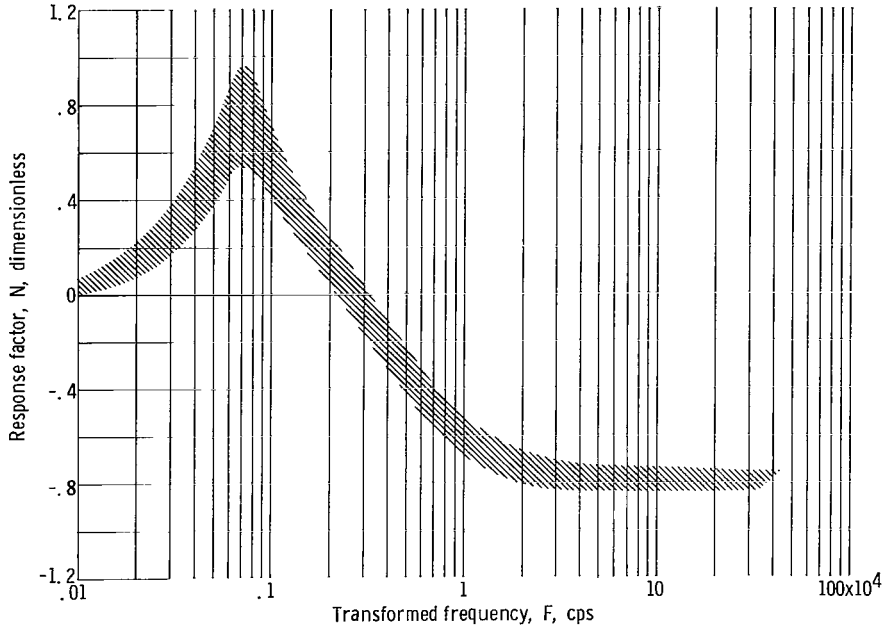


Figure 13. - Deviation from single curve in correlation of all results.

sure and velocity oscillations which may differ substantially. An effect on frequency response is expected.

## ANALYSIS OF RESULTS

The effect of boundary conditions on the frequency response of the vaporization process is, in most instances, characterized by a frequency displacement of the response curve. This forms the basis of the correlation in figure 12. An alternative treatment of the data is to relate the response factor to the characteristic times of the processes involved. These times are the lifetimes (or half-lifetimes) of the vaporizing drop and the wavetime of the oscillation. Figure 14 shows the response factor as a function of the ratio of drop half-lifetime to wave or cycle time. The correlation obtained is qualitatively equivalent to that of figure 12. Peak and zero values of the response factor occur at

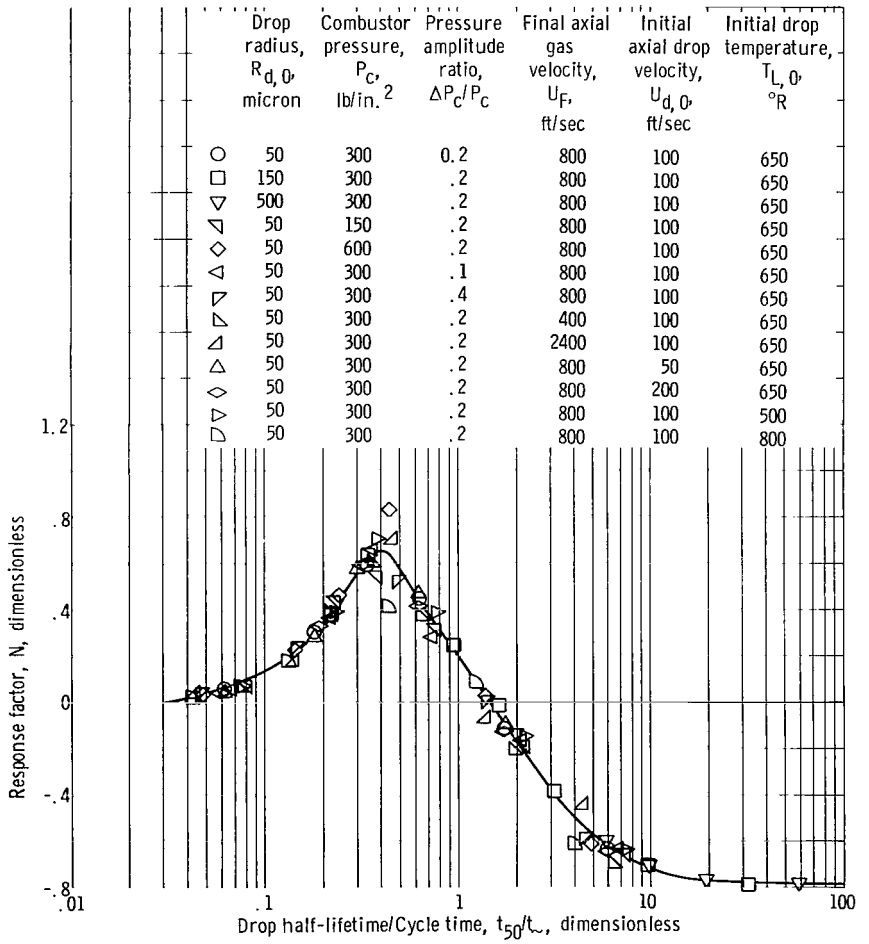


Figure 14. - Correlation of representative results with dimensionless time.

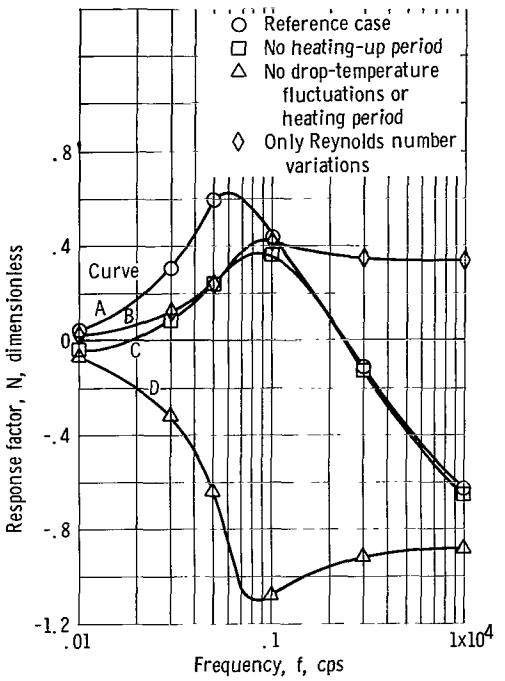


Figure 15. - Effect of restrictions on drop behavior. Drop conditions: radius, 50 microns; velocity, 100 feet per second; temperature, 650° R for reference case, 840° R for all others; radial position, 0.707 of combustor radius. Gas conditions: pressure, 300 pounds per square inch; final velocity, 800 feet per second; oscillation peak-to-peak amplitude, 0.2 of average gas pressure.

dimensionless times of about 0.4 and 1.4, respectively. This means that the response factor is near a maximum when the entire drop lifetime equals the oscillation period and negative when the lifetime is greater than three times the period.

In an attempt to relate specific characteristics of the response curve to their causes, detailed time variations in vaporization parameters were examined in several drop histories. In addition, calculations were made in which the behavior of the drop was restricted by holding terms in the vaporization equations constant. The results are shown in figure 15, with an unrestricted reference case for comparison.

The response factor (fig. 14) is negative when vaporization time is large compared with cycle time, and thus, many oscillations occur in the vaporization history. In this region, the thermal inertia of the drop is high relative to the oscillation frequency, and the mean drop temperature rises from its injection value to the equilibrium temperature with only a small oscillatory component. The mass transfer can be related to the pressure parameter

$$\dot{w} \sim \ln\left(\frac{P_T}{P_T - P_L}\right) \tag{17}$$

where the vapor pressure at the drop surface $P_L$ is constant for a constant temperature. Under these conditions, this analytic form predicts a decrease in vaporization rate with an increase in pressure, and it is the cause of negative response when drop lifetime is large. This is illustrated in figure 15, curve D, for computations in which drop temperature is held constant at the equilibrium value. The response factor is negative for all frequencies.

As drop lifetime approaches the period of oscillation, the drop temperature can respond to the acoustic oscillations. This favors mass transfer in phase with pressure and results in a peak positive response factor.

The elimination of the heating period by the injection of the drop at the equilibrium temperature (fig. 15, curve C) is amenable to the interpretation just given. At high frequencies, the heating period is relatively unimportant, because the drop temperature

changes very little during one cycle of oscillation throughout its lifetime. By the previous consideration, the response factor is negative for this condition and nearly identical to a drop with a heating period (curve A). In contrast, the heating period affects the response of a drop with a lifetime nearly equal to the cycle time. Gains during this heating period are larger than at equilibrium temperature and contribute to an increase in overall gain. The peak positive response factor, therefore, is largest for a drop with a heating period. The effect of initial temperature on response factor (fig. 8) results from a change in the heating period.

When drop lifetime is very small compared with cycle time, the response factor tends toward zero. In this region, the pressure and transverse gas velocities are essentially constant during the drop lifetime. In the limit of very small drops, the propellant is consumed as fast as it is injected regardless of chamber conditions. This gives a response factor of zero.

Variations of $\rho \Delta V$ in the Reynolds number also cause mass transfer perturbations. Velocity difference appears as a rectified function with almost identical curves over both half cycles of oscillation. Density, however, is in phase with pressure, and the product $\rho \Delta V$ produces only in-phase perturbations between mass transfer and pressure. This gives a positive response factor, as shown by curve B, where only the Reynolds number in the vaporization equation was allowed to vary.

The drop acquires transverse velocity components because of acceleration by transverse gas velocities. The phase between the transverse gas and drop velocities affects the phase and magnitude of $\Delta V$, especially for small, easily accelerated drops. To test the significance of this effect, curves B, C, and D of figure 15 were recalculated with transverse drop velocity held at zero. No appreciable change occurred in the shapes of the curves for the conditions examined.

## APPLICATION OF RESULTS

The application of the response characteristics of the vaporization process to combustor design may be approached in several ways. According to the correlation parameter of figure 12, a stable design with the response factor less than zero requires that

$$f\left(\frac{R_{d,0}}{50}\right)^{3/2}\left(\frac{300}{P_c}\right)^{1/3}\left(\frac{800}{U_F}\right)^{1/3}\left(\frac{0.2}{\frac{\Delta P_c}{P_c}}\right)^{1/3} > 2500 \qquad (18)$$

The frequency of oscillation is related to the combustor radius and the speed of sound by the relation (ref. 4)

$$f = 0.293 \frac{a}{R_w} \tag{19}$$

If an average speed of sound of 4250 feet per second is assumed for hydrocarbon and oxygen combustion products, the criterion for a zero response factor becomes

$$\left(\frac{0.5}{R_w}\right)\left(\frac{R_{d,0}}{50}\right)^{3/2}\left(\frac{300}{P_c}\right)^{1/3}\left(\frac{800}{U_F}\right)^{1/3}\left(\frac{0.2}{\frac{\Delta P_c}{P_c}}\right)^{1/3} > 1.0 \tag{20}$$

As a scaling parameter for $R_w$ and $R_{d,0}$, equation (20) states that the drop-size ratio must increase by the 2/3 power of the combustor radius to hold the response factor constant. When combustor thrust level increases by the square of the combustor radius, the drop size must increase by the 1/3 power of the thrust-level ratio. The other parameters in equation (20) may be examined for scaling in a similar manner.

In some applications, the combustor length required to vaporize or burn the propellants may be a design parameter that is more convenient to use than the vaporization paramater in equation (20). An approximate stability criterion involving the vaporization length can be formulated from the dimensionless time correlation (fig. 14, p. 19). This correlation predicts a response factor less than zero when

$$\frac{t_{50}}{t_\sim} > 1.4 \tag{21}$$

The dimensionless time can be transformed into a parameter ratio involving vaporization length from the following manner.

The oscillation period is related to the combustor radius, as in equation (19),

$$t_\sim = 3.41 \frac{R_w}{a} \tag{22}$$

The length to vaporize 50 percent of the drop weight $L_{50}$ is equal to the product of the drop half-lifetime and an average drop velocity, so that

$$t_{50} = \frac{L_{50}}{\bar{U}_d} \tag{23}$$

The drop velocity (from a generalization of vaporization histories) is assumed to increase linearly with combustor length to a final value equal to 80 percent of the final gas velocity. This gives an average value of 20 percent of the final gas velocity during the half-lifetime of the drop. Final gas velocity or Mach number is related to the combustor contraction ratio $\mathscr{A}$. This relation leads to the approximate equation

$$t_{50} = 7.7 \frac{L_{50}\mathscr{A}}{a} \tag{24}$$

When equations (22) and (24) are combined, the expression for dimensionless time is

$$\frac{t_{50}}{t_\sim} = 2.26\left(\frac{L_{50}}{R_w}\right)\mathscr{A} \tag{25}$$

When combined with equation (21), this criteria for a negative response factor is

$$\left(\frac{L_{50}}{R_w}\right)\mathscr{A} > 0.6 \tag{26}$$

Equation (26) states that $L_{50}/R_w$ must remain constant when scaling at constant contraction ratios and increase with any decrease in contraction ratio. This conflicts with general practice. Large combustors of high thrust are usually designed with smaller contraction ratios and aspect (length-to-diameter) ratios than small combustors of low thrust. This prescribes a lower value of $L_{50}/R_w$ for high-thrust combustors than the low-thrust combustors when the performance-length relation is maintained similar. In practice, therefore, the high-thrust combustors may be expected to have smaller values of $(L_{50}/R_w)\mathscr{A}$ than low-thrust combustors. This could lead to positive response factors and greater instances of instability in high-thrust combustors when the value of $(L_{50}/R_w)\mathscr{A}$ is near the critical value of 0.6.

The value of $(L_{50}/R_w)\mathscr{A}$ for some hydrocarbon and oxygen combustors of high thrust, which experienced transverse instability, can be computed from the data in reference 8. These are shown in figure 16. Stable and unstable configurations are plotted on the response curve, to show both $(L_{50}/R_w)\mathscr{A}$ and the expected value of the response factor. Figure 16 shows that these high-thrust combustors are in the region where in-

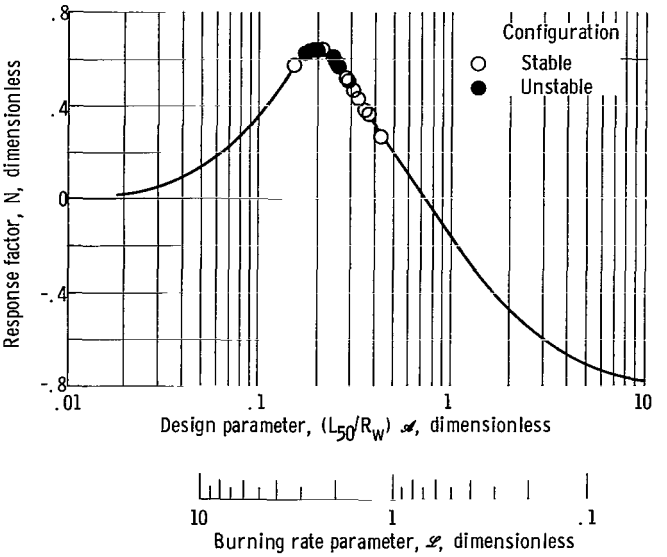


Figure 16. - Response factor related to combustor variables.

stability is most probable for a vaporization-limited combustion process.

The correspondence between $(L_{50}/R_w)\mathscr{A}$ and the burning rate parameter $\mathscr{L}$, used in the stability analyses of references 1, 2, and 8, is also shown in figure 16. They are related by the expression

$$\frac{1}{\mathscr{L}} = \frac{\mathscr{A}}{\dot{m}R_w} = 2\left(\frac{L_{50}}{R_w}\right)\mathscr{A} \tag{27}$$

when $\dot{m}$, the weight fraction vaporized per unit combustor length, is equated to $0.5/L_{50}$. Relating the response factor to $\mathscr{L}$, as in figure 16, adds a new dimension to interpreting the stability criteria presented in references 1 and 2. The response characteristics of the vaporization model used in these studies depended only on Reynolds number variations (fig. 15, curve D) and did not give a negative response region.

## COMPARISON WITH CHARACTERISTIC TIME AND INTERACTION INDEX

It is postulated in reference 7 that the combustion process in a rocket combustor may be characterized by two parameters, a characteristic time $\tau$ and an interaction index n. System stability is analyzed by using these parameters, and stability limits are analytically predicted for a variety of system boundary conditions. Such a characterization of the combustion process can be used to approximate the response of the vaporization process over a limited range of frequencies.

The expression for the fractional change in burning rate in terms of the characteristic time and interaction index is given in reference 6 as

$$\frac{\dot{w} - \bar{\dot{w}}}{\bar{\dot{w}}} = n\left[\frac{\tilde{P}_c - P_c}{P_c}(t) - \frac{\tilde{P}_c - P_c}{P_c}(t - \tau)\right]$$

where burning rate and vaporization rate are considered to be identical. If a sinusoidal pressure oscillation with time is assumed, the response factor (eq. (13)) for this functional form can be analytically evaluated and is given by

$$N = n(1 - \cos 2\pi f\tau) \tag{27}$$

This response function has a peak value of 2n at a frequency $f_{peak}$ equal to $1/2\tau$ cps. The peak amplitude of the response factor obtained from the average curve through the correlated vaporization results in figure 13 (p. 18) was about 0.74, which corresponds to an n equal to 0.37. This peak occurred at a transformed frequency value $F_{peak}$ of 750 cps. This value may be related to $f_{peak}$ by the frequency factor (eq. (16)) to give the following expression for characteristic time:

$$\tau = \frac{1}{2f_{peak}} = \frac{1}{1500}\left(\frac{R_{d,0}}{50}\right)^{3/2}\left(\frac{300}{P_c}\right)^{1/3}\left(\frac{800}{U_F}\right)^{1/3}\left(\frac{0.2}{\frac{\Delta P_c}{P_c}}\right)^{1/3} \tag{28}$$

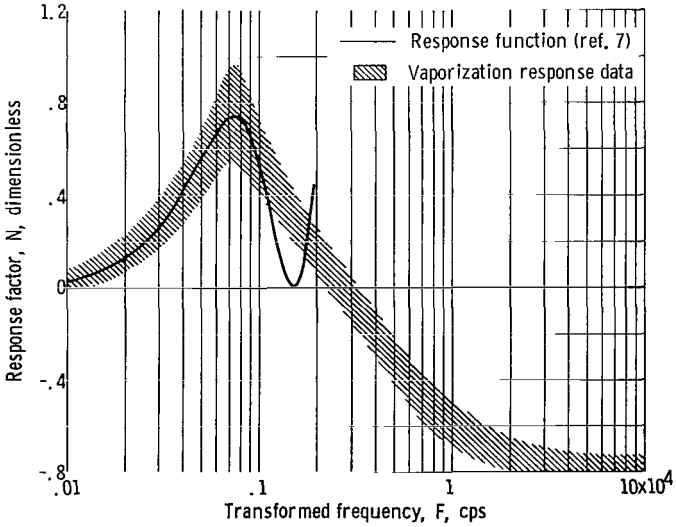


Figure 17. - Comparison of frequency response of vaporization process with function containing characteristic time and interaction index.

Setting n equal to 0.37, using equation (28) for $\tau$, and relating f to F again by equation (16), give the response curve shown in figure 17. It is seen that this response function approximates the low frequency portion of the response curve of the vaporization process.

Another general expression for characteristic time may be obtained from the correlation parameter dimensionless time $t_{50}/t_{\sim}$. Figure 14 (p. 19) shows that the response factor peaks at a dimensionless time equal to 0.4. By the inverse relation between

wave time and frequency,

$$\tau = \frac{1}{2}\left(\frac{t_{50}}{0.4}\right) \tag{29}$$

An interaction index of 0.37 is in general agreement with what has been postulated for the combustion process in liquid propellant combustors. A decrease in characteristic time with a decrease in drop size and an increase in combustor pressure as given by equation (28) or, more generally, a characteristic time proportional to the time to burn has been anticipated in liquid propellant combustors.

It may be concluded from this discussion that the response of the vaporization process may be partially approximated by a characteristic time and an interaction index and used to establish stability limits of systems previously analyzed with these parameters.

## SUMMARY OF RESULTS

The frequency response of the vaporization process was evaluated from an analysis of drop vaporization in a combustor with superimposed traveling transverse acoustic oscillations. The response is expressed as the ratio of the percentage oscillation in vaporization rate in phase with pressure to the percentage oscillation in pressure. The following results were obtained:

1. A typical response curve attained a peak value at a specific frequency. It decreased to zero at lower frequencies and to a constant negative value at higher frequencies.

2. Frequency response characteristics were related to a dimensionless time, which is the ratio of the time required to vaporize 50 percent of the drop mass to the period of the oscillation. Peak response occurred at a dimensionless time of 0.4. Negative gain occurs at dimensionless times greater than 1.4.

3. Frequency response curves for heptane were correlated by a transformed frequency factor. The factor at the critical condition for zero response factor is

$$\frac{2500}{f} = \left(\frac{R_{d,0}}{50}\right)^{3/2}\left(\frac{300}{P_c}\right)^{1/3}\left(\frac{800}{U_F}\right)^{1/3}\left(\frac{0.2}{\frac{\Delta P}{P_c}}\right)^{1/3}$$

where $R_{d,0}$ is the drop radius, $P_c$ is the combustor pressure, $U_F$ is the final axial

gas velocity, and $\Delta P/P_c$ is the pressure amplitude ratio. Two other parameters examined, initial drop velocity and temperature, had a small effect on the critical frequency dividing regions of positive and negative gain.

4. The characteristics of the frequency response curves were physically related to the temperature of the drop. A large oscillating component in drop temperature gave a positive response factor, while a drop without temperature oscillations gave a negative response factor. Reynolds number variations always contributed to a positive response factor.

5. Calculations for oxygen vaporization showed propellant properties to affect frequency response. The peak value and corresponding frequency required for the peak value of the response factor were significantly higher than for heptane. No region of negative gain occurred for oxygen.

6. A comparison of results with combustor design practices implied that instability is more probable in high-thrust combustors than in low-thrust combustors.

7. A comparison of analytical and experimental results showed that unstable combustor designs are in the region where instability is most probable for a vaporization-limited combustion process.

8. The response of the vaporization process may be partially approximated by a characteristic time and interaction index previously used to characterize the combustion process in system stability analysis.

Lewis Research Center,
National Aeronautics and Space Administration,
Cleveland, Ohio, February 14, 1966.

## REFERENCES

1. Priem, Richard J.: and Guentert, Donald C.: Combustion Instability Limits Determined by a Nonlinear Theory and a One-Dimensional Model. NASA TN D-1409, 1962.

2. Priem, Richard J.: Influence of Combustion Process on Stability. NASA TN D-2957, 1965.

3. Priem, Richard J.; and Heidmann, Marcus F.: Propellant Vaporization as a Design Criterion for Rocket-Engine Combustion Chambers. NASA TR R-67, 1960.

4. Morse, Philip M.: Vibration and Sound. 2nd Ed., McGraw-Hill Book Co., 1948.

5. Mickelsen, William R.: Effect of Standing Transverse Acoustic Oscillations on Fuel-Oxidant Mixing in Cylindrical Combustion Chambers. NACA TN 3983, 1957.

6. Wieber, Paul R.: Calculated Temperature Histories of Vaporizing Droplets to the Critical Point. AIAA J., vol. 1, no. 12, Dec. 1963, pp. 2764-2770.

7. Crocco, Luigi; and Cheng, Sin-I: Theory of Combustion Instability in Liquid Propellant Rocket Motors. AGARDograph No. 8, Butterworths Scientific Publications, Ltd., London, 1956.

8. Priem, Richard J.; and Morrell, Gerald: Application of Similarity Parameters for Correlating High Frequency Instability Behavior of Liquid Propellant Combustors. Detonation and Two-Phase Flow, vol. 6 of Progress in Astronautics and Rocketry. S. S. Penner and F. A. Williams, eds., Academic Press, 1962, pp. 305-320.

*"The aeronautical and space activities of the United States shall be conducted so as to contribute . . . to the expansion of human knowledge of phenomena in the atmosphere and space. The Administration shall provide for the widest practicable and appropriate dissemination of information concerning its activities and the results thereof."*

—NATIONAL AERONAUTICS AND SPACE ACT OF 1958

# NASA SCIENTIFIC AND TECHNICAL PUBLICATIONS

TECHNICAL REPORTS: Scientific and technical information considered important, complete, and a lasting contribution to existing knowledge.

TECHNICAL NOTES: Information less broad in scope but nevertheless of importance as a contribution to existing knowledge.

TECHNICAL MEMORANDUMS: Information receiving limited distribution because of preliminary data, security classification, or other reasons.

CONTRACTOR REPORTS: Technical information generated in connection with a NASA contract or grant and released under NASA auspices.

TECHNICAL TRANSLATIONS: Information published in a foreign language considered to merit NASA distribution in English.

TECHNICAL REPRINTS: Information derived from NASA activities and initially published in the form of journal articles.

SPECIAL PUBLICATIONS: Information derived from or of value to NASA activities but not necessarily reporting the results of individual NASA-programmed scientific efforts. Publications include conference proceedings, monographs, data compilations, handbooks, sourcebooks, and special bibliographies.

***Details on the availability of these publications may be obtained from:***

**SCIENTIFIC AND TECHNICAL INFORMATION DIVISION**

**NATIONAL AERONAUTICS AND SPACE ADMINISTRATION**

**Washington, D.C. 20546**